AD_____

Award Number: DAMD17-00-1-0278

TITLE: Involvement of Heparanase in Breast Carcinoma Progression

PRINCIPAL INVESTIGATOR: Israel Vlodavsky, Ph.D.
Yael Friedmann, Ph.D.
Tamar Peretz, M.D.

CONTRACTING ORGANIZATION: Hadassah Medical Organization
Jerusalem, Israel 91120

REPORT DATE: June 2002

TYPE OF REPORT: Annual

PREPARED FOR: U.S. Army Medical Research and Materiel Command
Fort Detrick, Maryland 21702-5012

# REPORT DOCUMENTATION PAGE

Form Approved
OMB No. 074-0188



| 1. AGENCY USE ONLY (Leave blank) | 2. REPORT DATE | 3. REPORT TYPE AND DATES COVERED |
|---|---|---|
| | June 2002 | Annual (1 Jun 01 - 31 May 02) |

**4. TITLE AND SUBTITLE**
Involvement of Heparanase in Breast Carcinoma Progression

**5. FUNDING NUMBERS**
DAMD17-00-1-0278

**6. AUTHOR(S)**
Israel Vlodavsky, Ph.D.
Yael Friedmann, Ph.D.
Tamar Peretz, M.D.

**7. PERFORMING ORGANIZATION NAME(S) AND ADDRESS(ES)**
Hadassah Medical Organization
Jerusalem, Israel 91120

E-mail: Vlodavsk@cc.huji.ac.il

**8. PERFORMING ORGANIZATION REPORT NUMBER**

**9. SPONSORING / MONITORING AGENCY NAME(S) AND ADDRESS(ES)**
U.S. Army Medical Research and Materiel Command
Fort Detrick, Maryland 21702-5012

**10. SPONSORING / MONITORING AGENCY REPORT NUMBER**

**11. SUPPLEMENTARY NOTES**
Report contains color



**12a. DISTRIBUTION / AVAILABILITY STATEMENT**
Approved for Public Release; Distribution Unlimited

**12b. DISTRIBUTION CODE**

**13. ABSTRACT** *(Maximum 200 Words)*

Cellular localization of heparanase was found to be a major determinant of its pro-metastic and pro-angiogenic properties. While normally, the human enzyme is localized mostly in late endosomes and lysosomes, both the cellular content and secretion of heparanase were stimulated by estrogen. Estrogen may thus promote breast cancer progression through stimulation of heparanase transcription and secretion. Processing and activation of latent hehparanase by MDA-435 breast carcinoma cells was inhibited by maspin, but not by BBI (Bowman-Birk inhibitor). BBI was applied to increase the yield of active heparanase, since it efficiently inhibited degradation of the enzyme by cellular proteases. Primary tumors produced by MCF-7 breast carcinoma cells over-expressing a secreted form of heparanase, elicited a potent angiogenic response and grew faster than tumors produced by MCF-7 cells expressing the intracellular enzyme. Mammary glands of pregnant transgenic mice over-expressing heparanase exhibited a massive branching of ducts, hyperplasia and basement membrane (BM) disruption, associated with intense neovascularization of the mammary tissue. We applied a ribozyme targeting approach to suppress heparanase expression in MDA-435 breast carcinoma cells. A pronounced inhibition of heparanase activity and BM invasion was obtained. We identified lead species of heparin and laminaran sulfate that efficiently inhibit the enzyme. Our results further emphasize the involvement of heparanase in breast carcinoma progression.

**14. SUBJECT TERMS**
heparanase, heparan sulfate, metastasis, angiogenesis, gene expression, breast cancer

**15. NUMBER OF PAGES**
22

**16. PRICE CODE**

| 17. SECURITY CLASSIFICATION OF REPORT | 18. SECURITY CLASSIFICATION OF THIS PAGE | 19. SECURITY CLASSIFICATION OF ABSTRACT | 20. LIMITATION OF ABSTRACT |
|---|---|---|---|
| Unclassified | Unclassified | Unclassified | Unlimited |

## Table of Contents

## Introduction

Metastases formation depends on the ability of tumor cells to invade basement membranes (BM) and tissue barriers in a process involving enzymes capable of degrading extracellular matrix (ECM) components. While the majority of studies focus on proteolytic enzymes and their inhibitors, the involvement of glycosaminoglycan (GAG) degrading enzymes (e.g., heparanase) was underestimated. The overall goal of the proposed research is to study the involvement of heparanase (heparan sulfate degrading endoglycosidase) in breast carcinoma metastasis and angiogenesis. For this purpose, we proposed to determine the effect of increased heparanase expression on breast carcinoma progression in non-metastatic human and mouse breast cancer cells (task 1). An increased expression of the enzyme was also achieved *in vivo* by producing transgenic mice over-expressing the heparanase RNA and protein in all tissues and analyzing the resulting effect on morphogenesis, growth and hyperplasia of mammary epithelial cells. In an attempt to better elucidate the regulation of heparanase gene expression, we proposed to construct a vector composed of the heparanase promoter fused to a luciferase reporter gene and study the effect of estrogenes and anti-estrogens on its expression and cellular localization in transfected breast carcinoma cells (task 2). A related aspect was to study the processing and activation of latent heparanase by highly metastatic breast carcinoma cells, toward characterization and purification of a putative heparanase converting protease (task 1b). Finally, we proposed to prepare and characterize heparanase-inhibiting molecules, primarily define species of laminaran sulfate, and evaluate their effect on heparanase activity *in vitro* and breast carcinoma metastasis and angiogenesis *in vivo*. We also investigated the effect of RNA molecules with heparanase sequence-specific endonucleolytic activity (task 3).

## Body

### Task 1: Involvement of heparanase in breast cancer metastasis and angiogenesis

**Processing and activation of latent heparanase.** The heparanase gene encodes a latent 65 kDa proenzyme that is processed at the N-terminus into a highly active 50 kDa enzyme. The proteolytic cleavage of the 65 kDa proenzyme is likely to occur in two potential cleavage sites, $Glu^{109}$-$Ser^{110}$ and $Gln^{157}$-$Lys^{158}$, yielding an 8 kDa polypeptide at the N-terminus, a 50 kDa polypeptide at the C-terminus and a linker polypeptide in between them (1). This proteolytic cleavage is essential for obtaining functional heparanase. Several human breast carcinoma cell lines (MCF-7; MDA-231; MDA-435) were tested for their ability to process and activate the heparanase enzyme. Best results in terms of processing and gain of heparanase activity were obtained with the highly metastatic MDA-435 cells, using either a cytosol (Fig. 1) or cell membrane (Fig. 2) fractions. Incubation of the 65 kDa enzyme with each of these preparations yielded excess degradation into low molecular weight peptides. As demonstrated in figure 3, addition of BBI (Bowman-Birk soybean derived serine protease inhibitor) (1) prevented this undesirable degradation, but had no effect on conversion of the latent enzyme into the active 50 kDa heparanase. On the basis of this result and in order to improve the yield and purity of the processed 50 kDa

enzyme, BBI is included during subsequent characterization and purification steps of the heparanase converting protease.

Maspin (mammary serine protease inhibitor) was originally identified as a tumor suppressor protein in human breast epithelial cells and is a member of the serine proteases inhibitor (serpin) superfamily (2). It inhibits tumor cell motility and angiogenesis and its down-regulation is associated with the development of breast cancers. Overexpression of maspin in transgenic mice could partially block mammary tumor progression. Moreover, maspin was shown to block tumor growth, invasion and metastasis in a syngeneic breast cancer model (2). In a search for an efficient inhibitor of heparanase processing and activation, we have tested the effect of maspin on the ability of MDA-435 cells to convert the heparanase enzyme from a latent 65 kDa form into an active 50 kDa enzyme. Complete inhibition was obtained, suggesting that the anti-cancerous effect of maspin may be attributed, in part, to its inhibition of heparanase processing and activation (Fig. 3).

**Overexpression of secreted heparanase accelerates tumor growth and promotes tumor angiogenesis.** We have produced a chimeric construct composed of the chicken heparanase signal peptide preceding the human heparanase cDNA. Cells transfected with this construct exhibited cell surface localization and secretion of the enzyme, as opposed to a mostly intracellular localization and little or no secretion of the human enzyme (4). Applying both histological analysis of vascular density in tissue sections and non-invasive MRI for *in vivo* mapping of vascular density, maturation and functionality in the primary tumor (5), we have recently demonstrated a remarkable pro-angiogenic response to lymphoma cells over-expressing the secreted form of heparanase (6). In comparison, lymphoma cells expressing the enzyme mostly intracellularly elicited a modest angiogenic response. The pro-angiogenic effect of heparanase was also reflected by stimulated tissue vascularity, granulation and wound repair in response to exogenously added recombinant heparanase (7).

**Vascular density, functionality and maturation.** As proposed in the previous progress report, we compared the tumorigenicity of MCF-7 cells over-expressing the human enzyme (H-*hpa*) to cells transfected with secreted forms of heparanase (Chk-*hpa;* Chimeric *hpa*). Briefly, primary tumors produced by MCF-7 cells expressing the secreted and non-secreted species of heparanase were compared in real time for their vascular functionality and maturation. For this purpose, tumor-bearing mice were subjected to magnetic resonance imaging (MRI) on day 30 after cell inoculation. The size of the primary tumor was higher (3-4-fold) in mice inoculated with MCF-7 cells expressing the secreted (Chk-*hpa)*, vs. the mostly intracellular (H-*hpa)* heparanase enzyme (Fig. 4, left panels). Functionality and maturation of the neovasculature were determined from gradient echo images acquired during the inhalation of air, air-$CO_2$, and oxygen-$CO_2$ (5). The rational for this approach is that vessels coated with pericytes and smooth muscle cells, in contrast with immature endothelial capillaries, respond to hypercapnia (elevated $CO_2$) by vasodilatation, while all functional blood vessels show a change in hemoglobin saturation in response to hyperoxia (elevated $O_2$), reflecting the capacity of erythrocytes to deliver inhaled oxygen to the

tumor vasculature. Both vasodilatation and changes in hemoglobin saturation are detected by gradient echo imaging using the intrinsic contrast generated by changes in deoxyhemoglobin, blood volume and blood flow (5,6). As shown in figure 4, there was a significant elevation in vascular functionality (VF) in tumors produced by MCF-7 cells over-expressing the Chk-*hpa*, vs. those produced by H-*hpa* transfected cells (Fig. 4A, VF; Fig. 4B). Maturation of the tumor vasculature appeared to proceed from the margins of the tumor inward, regardless of the inoculated cell type. However, a higher degree of vessel maturation (vasodilatation, VD) was observed in the center of tumors generated by Chk-*hpa*- vs. H-*hpa*- transfected cells (Fig. 4A, VD; Fig. 4B).
The high vascularity of tumors produced by MCF-7 cells expressing the secreted (Chimeric-*hpa*) (Fig. 5B-D) vs. the non-secreted (H-*hpa*) (Fig. 5A) enzyme was also demonstrated by histological examination of the respective tissue sections. Intense neovascularization (high vascular density) was seen in the vicinity of tumors produced by MCF7 cells expressing the secreted enzyme vs. little or no angiogenesis of tumors produced by cells expressing the mostly intracellular human heparanase. These results indicate that cell surface expression and secretion of heparanase in breast cancer cells markedly promote tumor angiogenesis and vascular maturation.

**Task 2: Control of heparanase gene expression**

**Effect of estrogen on heparanase expression, cellular content, localization and secretion.** Quantitative RT-PCR revealed a 4-fold increase in heparanase mRNA following treatment (24 h) of estrogen-depleted MCF-7 cells with 1 nM estrogen. This increase was abolished in the presence of the estrogen antagonist ICI128 (Fig. 6). Estrogen had no effect on heparanase RNA expression in estrogen receptor (ER) negative MDA231 breast carcinoma cells (Fig. 6). These experiments were performed in collaboration with Drs. Hynda Kleinman and Michael Elkin (NIDR, NIH).

It has been previously reported that estradiol increases the secretion of procathepsin-D and other lysosomal enzymes in estrogen receptor (ER)-positive breast cancer cells (9). Estradiol also increased the expression of cathepsin-D and decreased the levels of Man-6-P/IGF-II receptor mRNA and protein (10). It was proposed that Man-6-P/IGF-II receptor becomes saturated after estradiol treatment, leading to estrogen-induced secretion of procathepsin-D and other lysosomal proenzymes that are routed by the same transport system (10). Derouting and increased secretion of lysosomal proteases have also been described for cathepsin-B in melanoma and cathepsin-L in 3T3-transformed fibroblasts, suggesting that this alteration may be general in cancer cells, where it might play a role in facilitating cell invasion and metastasis. As reported in our previous progress report, both heparanase promoter activity (applying luciferase reporter gene) and gene expression (RT-PCR) (Fig. 6A) were stimulated by estrogen in MCF-7 cells. There was no effect on estrogen receptor (ER) negative MDA-231 cells (Fig. 6B). These findings and the localization of heparanase in late endosomes and lysosomes (see below), suggest that a similar control mechanism may lead to increased secretion of heparanase by estradiol. To investigate this possibility, MCF-7 cells, expressing a very small amount of intracellular heparanase and no secretion of the enzyme were transfected with secreted and membrane associated species of heparanase (i.e., Chk-*hpa*; Chimeric-*hpa*). Stable transfected

cells were pretreated with estradiol (2h, 1 x $10^{-8}$ M) and their serum free conditioned medium analyzed for heparanase activity. As demonstrated in figures 7A and 7B, exposure to estradiol resulted in a marked stimulation of heparanase secretion into the culture medium. Under the same experimental conditions, there was little or no effect of estradiol on secretion of heparanase by mock-transfected MCF-7 cells (Fig. 7A), or cells transfected with the non-secreted human enzyme (not shown). Immunostaining of heparanase revealed a marked increase in the cellular content of heparanase in response to pretreatment with estradiol (Fig. 7B). Estradiol exerted little or no effect in mock-transfected MCF-7 cells (Fig. 7B). This result corroborates our previous observation on the up-regulation of heparanase gene expression in estradiol treated cells. Altogether, these results suggest that estrogen efficiently up-regulates both heparanase expression and secretion. Interestingly, estrogen also stimulated angiogenesis induced *in vivo* by MCF-7 cells embedded in a Matrigel gel (Matrigel plug assay) (Fig. 8).

**Cellular localization of heparanase.** In view of the significance of heparanase cellular localization and secretion, MCF-7 and MDA-231 breast carcinoma cells expressing endogenous heparanase were subjected to transmission electron microscopy (TEM) and immuno-gold labeling of heparanase. Specific heparanase labeling was detected within lysosomes (Fig. 9A & B, arrows) and the Golgi apparatus (Fig. 9C, arrow) of these cells. A similar distribution pattern was observed in transfected MCF-7 cells over-expressing the heparanase enzyme (not shown). Heparanase labeling was also noted in coated pits of MDA-231 cells (Fig. 9D).

We have also examined heparanase localization applying immunofluorescence. For this purpose, non-metastatic (MCF-7) and moderately metastatic (MDA-231) human breast carcinoma cells were immunostained with anti-heparanase mAb 130. A perinuclear granular staining was observed in both MCF-7 (Fig. 10A, left) and MDA-231 (Fig. 10B, left). Staining of living MCF-7 and MDA-231 cells with LysoTracker yielded the same cytoplasmic granular staining pattern (Fig. 10 A&B, middle), as also indicated by the co-localization of heparanase and LysoTracker observed in double stained cells (Fig. 10 A&B, right). In both the MCF-7 and MDA-231 cells, the cytoplasm is occupied mostly by the nucleus.

**Heparanase activity depends on the integrity of the Golgi apparatus.** In order to examine whether heparanase trafficking via the Golgi is essential for its proper maturation, MCF7 and MDA-231 cells were treated with Brefeldin A (BFA), a drug which dissociates the coat proteins from the trans-Golgi membranes, resulting in disassembly of the Golgi (11). Briefly, cells were preincubated (16 h, $37^0$C) with BFA and examined for their heparanase activity. Untreated cells were used as control. As shown in figure 11A, heparanase activity was reduced (3-5 fold) in MCF7 cells treated with 0.1-10 μg/ml of the drug. A similar inhibition was obtained with MDA-231 cells treated with 1-5 μg/ml BFA (Fig. 11B). BFA had no inhibitory effect on heparanase activity when incubated directly with purified heparanase, or when BFA treated cells were lysed and incubated with the recombinant enzyme (not shown).

**Involvement of heparanase in branching morphogenesis and hyperplasia of the mammary gland.** An intact basement membrane (BM) is essential for the proper function, differentiation and morphology of many epithelia. Disruption or loss of this BM occurs during normal development of the mammary gland, as well as during breast carcinoma progression. To investigate the involvement of heparanase in mammary gland remodeling, differentiation and transformation, we generated transgenic mice over-expressing the heparanase cDNA and protein in all tissues (12). As reported previously, examination of mammary glands taken from normal virgin females revealed the typical branching pattern. Morphological evaluation of whole-mount preparations from 2-3 month old virgin homozygous transgenic mice, revealed abnormally abundant side branches and precocious alveolar structures with primary and secondary ducts (12). It was also noted that the circumference of many of the mammary ducts was wider in the transgenic mice compared to non-transgenic ones. We have now extended the characterization of this phenotype, focusing primarily on pregnant mice. As demonstrated in figure 12, the mammary gland ducts and alveoli of 14-day pregnant transgenic mice were very dense, the alveoli were abnormally clustered with high incidence of severe hyperplasia, and the ductal circumference was about 5 fold wider (Fig. 12A, arrows; Fig. 12A; bottom, right) compared with that of normal mammary ducts of control pregnant mice at this age (Fig. 12A, without arrows; Fig. 12A; top, right). Interestingly, heparanase activity was found in the milk obtained from two transgenic lines, 7-10 days after delivery. There was no activity in the milk of control mice.

The histology of the mammary glands was evaluated in tissue sections stained for BM components. Disruption of collagen in the BM surrounding the mammary ducts and alveoli of the transgenic mice was noted by Masson-trichrom staining (Fig. 12B). These results suggest that heparanase in the transgenic mammary gland is actively digesting the sub-epithelial BM/ECM and may thus allow branching, dense alveolar formation and widening of the ducts. Staining for heparanase, using newly developed polyclonal antibodies that recognize both the mouse and human enzymes, revealed that the enzyme is expressed in the mammary gland of control mice, albeit to a much lower extent as compared with *hpa*-transgenic mice (Fig. 12C). Over branching and hyperplasia of the mammary epithelium was associated with extensive neovascularization, as revealed by numerous blood vessels in close contact with the mammary ducts and alveoli (Fig. 12D; immunostaining with anti-SMC actin antibodies; anti-SMC actin antibodies also stained myoepithlelial cells along the alveolar structures and ducts). Abundant capillary vessels were seen when the same sections were stained with anti-CD31 antibodies (not shown). It appears that heparanase in the transgenic mammary gland is actively digesting the sub-epithelial BM/ECM and thus enable branching, dense alveolar formation and widening of the ducts. Cleavage of BM HSPGs by heparanase appears to unmask ECM molecules and liberate HS-bound growth promoting factors sequestered by heparan sulfate in the ECM, resulting in stimulation of cell proliferation and neovascularization (6).

**Task 3: Heparanase inhibitory molecules**

**Ribozyme.** We have applied a ribozyme (RNA molecule with sequence-specific endonucleolytic activity) targeting approach to suppress heparanase expression in cancer cells. The heparanase RNA was specifically cleaved by several ribozymes *in vitro* (Fig. 13A, left). A significant reduction in heparanase activity (Fig. 13A, middle) and Matrigel invasion (Fig. 13B) was also observed in cells (MDA435 breast carcinoma) expressing a high level of endogenous heparanase activity. Transient transfection of these cells with a cDNA encoding the most active anti-heparanase ribozyme (R8) resulted in a profound inhibition of their invasion through Matrigel as opposed to cells transfected with a control ribozyme (CRz, Fig. 13B).

**Species of heparin and laminaran sulfate.** The structure of heparin is largely accounted for by sequences of trisulfated disaccharide (TD) units made up of α-linked L-iduronic acid 2-sulfate and D-glucosamine N,6-disulfate, with minor sequences constituted by D-glucuronic and N-acetylated glucosamine residues. Inhibition of recombinant heparanase was determined for heparin derivatives differing in degrees of N-acetylation, 2-O-sulfation, and glycol-splitting of nonsulfated uronic acid residues. We have screened 35 species of heparin. Each compound was tested at several concentrations (0.2-25 μg/ml) for its ability to inhibit the heparanase enzyme using metabolically sulfate labeled ECM as a substrate. Within the unmodified heparin series, the strongest heparanase inhibitors were fractions with the highest content of TD sequences. N-desulfation/N-acetylation involved a progressive decrease in inhibitory activity. However, glycol splitting of nonsulfated uronic acid residues significantly increased this inhibitory activity, both for otherwise nonmodified heparins and for heparins 2-O-desulfated up to a total of about 50% of their uronic residues. Partially 2-O-desulfated and glycol split derivatives inhibited heparanase significantly more than the original heparins. Since glycol splitting also involves inactivation of the active site for antithrombin, these derivatives have very low anticoagulant activity. Our results are compatible with a tentative model in which the N-acetylated side of the heparin derivative is recognized by heparanase, while the fully sulfated side strongly binds to the enzyme. Relatively flexible polysulfated chains such as heparin and laminarin sulfate (LS) are expected to envelope the basic clusters of heparanase and compete with its binding to heparan sulfate. As candidate drugs, they are expected, however, to be poorly bioavailable since they are easily sequestered by tissues and induce unwanted side effect. On the basis of structure-activity relationship emerging from our inhibition studies, we have initiated a collaborative research with Dr. Benito Casu (G. Ronzoni Research Institute, Milan, Italy) aimed to remove sulfate groups not necessarily involved in enzyme recognition and inhibition. Our goal is to determine the minimal length of oligosaccharide and level of sulfation required for efficient inhibition of heparanase activity, tumor angiogenesis and metastasis. We plan to further improve the molecular flexibility and biological interactions of heparin and LS, applying controlled glycol-splitting and sulfation/desulfation strategies. We also plan to modify selected heparanase-inhibiting oligosaccharides by mimicking the critical heparanase cleavable glycosidic C-O-C bond with resistant C-S-C or C-C bonds. Modified oligosaccharides, prepared by the group of Dr. Casu, will be tested in our *in vitro* and *in vivo* experimental models.

In performing these experiments, we will apply transfected MCF-7 breast carcinoma cells over-expressing the secreted and membrane bound form of heparanase. Following s.c injection of these cells, tumor progression (growth rate, angiogenesis, metastasis, survival) is highly dependent on heparanase.

**Key research accomplishments**

**i)** Cellular localization of heparanase was found to be a major determinant in its involvement in breast cancer progression. Primary tumors produced by MCF-7 human breast carcinoma cells over-expressing a secreted form of heparanase elicited a potent angiogenic response (evaluated by MRI analysis of vascular functionality and maturation) and grew faster then tumors produced by MCF-7 cells expressing primarily the intracellular form of the enzyme.

**ii)** Localization studies, applying immunogold and immunofluoresence staining of heparanase in human breast carcinoma cells, revealed that the enzyme is localized mostly in late endosomes and lysosomes. Integrity of the Golgi apparatus was necessary for heparanase activity. Both the cellular content and secretion of heparanase were stimulated in response to pre-treatment with estrogen. Estrogen also stimulated heparanase promoter activity in estrogen positive breast cancer cells. These results indicate that estrogen may promote breast cancer progression through an effect on heparanase promoter activity and secretion of the enzyme.

**iii)** Processing and activation of the latent 65 kDa heparanase by MDA-435 breast carcinoma was inhibited by serine protease inhibitors (i.e., PMSF, DCI), but not by the Bowman-Birk soybean chemotrypsin-trypsin inhibitor (BBI). BBI was therefore applied to increase the yield and purity of the 50 kDa active heparanase, since it inhibited degradation of the active enzyme by cellular proteases. Maspin, a serine protease inhibitor which partially blocks mammary tumor progression, efficiently inhibited processing and activation of the heparanase enzyme.

**iv)** A ribozyme (RNA molecule with sequence-specific endonucleolytic activity) targeting approach was applied to suppress heparanase expression in MDA-435 breast carcinoma cells. A pronounced reduction in heparanase activity and basement membrane (Matrigel) invasion was observed in MDA-435 cells transfected with the appropriate ribozyme construct. We have also identified lead species of heparin and laminaran sulfate that efficiently inhibit the enzyme.

**v)** Mammary glands of pregnant transgenic mice over-expressing the heparanase enzyme exhibited intense branching of ducts, hyperplasia and basement membrane disruption, associated with abundant vascularization of the mammary tissue. This phenotype reflects the involvement of heparanase in mammary tissue morphogenesis, hyperplasia and vascularization.

**vi)** Our results indicate that heparanase expression, enzymatic activity and involvement in breast cancer progression are tightly regulated by its promoter activity, proteolytic processing, and cellular localization and secretion.

**Reportable outcomes**

**Manuscripts:**

Vlodavsky, I., and Friedmann, Y. Molecular properties and involvement of heparanase in cancer metastasis and angiogenesis. J. Clin. Invest. 108: 341-347, 2001.

Vlodavsky, I., Goldshmidt, O., Zcharia, E., Atzmon, R., Peretz, T., Elkin, M., and Friedmann, Y. Mammalian heparanase: Involvement of heparanase in cancer metastasis, angiogenesis and normal development. Seminars Cell Biol. 12: 121-129, 2002.

Vlodavsky, I., Goldshmidt, O., Zcharia, E., Metzger, S., Peretz, T., Pecker, I., and Friedmann, Y. Molecular properties and involvement of heparanase in cancer progression and normal development. Biochimie, 83: 831-839, 2001.

Goldshmidt, O., Nadav, L., Katz, B-Z. Yacoby-Zeevi, O., Zamir, E., Pecker, I., Geiger, B., Eldor, A., Cohen, I., and Vlodavsky, I. Human heparanase is localized within lysosomes in a stable form. Exptl. Cell Res. In revision.

**Presentations:**

Glyco XVI (the Hague, Aug. 2001)

53rd Harden Conference "Proteoglycans" (Aug. 2001; Ambleside UK)

ComBio 2001 (Canberra, Australia; October 2001)

Thrombosis & Hemostasis in Cancer (Bergamo, Itali; Nov. 2001)

7TH congress of the European Haematology Association (Florence, Italy, June 2002)

2nd International Conference on Tumor Microenvironment (Baden, Austria, June 2002)

**Conclusions**

Our research during the second year of research focused on each of the tasks stated in the original application, toward a better understanding of the involvement of heparanase in breast carcinoma progression. In particularly, we investigated parameters related to the regulation of heparanase expression and activity in breast cancer cells. Studies performed during the first year of research indicated that heparanase gene expression is up-regulated in response to estrogen at the transcriptional level (*task 2*). As expected, estrogen has no effect on receptor negative cells. We now report that estrogen also increases the cellular content and secretion of the enzyme, similar to its effect on cathepsin D in breast cancer cells. This finding led us to investigate in detail the cellular localization of heparanase, applying immunofluorescence and immunogold staining. We report that the enzyme is localized primarily in late endosomes and lysosomes and that the integrity of the Golgi apparatus is necessary for its enzymatic activity. A manuscript describing these results is being revised for publication. The mechanism by which estrogen affects heparanase routing and secretion is being investigated. This research is of particular significance in view of our recent *in vivo* studies showing that estrogen promotes angiogenesis (Matrigel plug assay) and that primary tumors produced by MCF-7 breast carcinoma cells over-expressing a secreted form of heparanase elicit a pro-angiogenic response and grew faster then tumors produced by MCF-7 cells expressing primarily the intracellular form of the enzyme (*task 1).* These results corroborate our impression, stated in the previous progress report, that translocation of heparanase from the cytoplasm to the cell surface plays an important regulatory role in affecting the involvement of the enzyme in both breast cancer progression and normal morphogenesis of the mammary gland. A detailed large scale *in vivo* experiment, addressing the effect of heparanase cellular localization and secretion on tumor growth and angiogenesis is being performed. As demonstrated in this progress report, tumor angiogenesis was evaluated by MRI analysis of vascular density, functionality and maturation, a non-invasive technique that, in our opinion, is more objective and informative than the previously applied histological examination of the tumor tissue. An intense angiogenic response was also noted in mammary glands from pregnant transgenic mice over-expressing the human enzyme. In order to study the significance of heparanase secretion in this system, we have already produced transgenic mice over-expressing a secreted form of heparanase. Homozygous females are being obtained and will soon be analyzed for the level of neovascularization and extent of branching and hyperplasia, in comparison with the currently available mice expressing the mostly intracellular enzyme.

Another regulatory element that was extensively studied during the past year is the proteolytic processing and activation of the 65 kDa pro-heparanase by MDA-435 breast cancer cells (*task 1).* We report that this processing can be inhibited by potent serine protease inhibitors (i.e., PMSF, DCI), but not by the Bowman-Birk soybean chymotrypsin-trypsin inhibitor (BBI). BBI is therefore being applied to increase the yield of the 50 kDa active heparanase during purification, using MDA-435 cells as a source, since it inhibits non-specific degradation of the active enzyme by cellular proteases. Interestingly, maspin, a serpin that partially blocks mammary tumor

progression, efficiently inhibits processing and activation of recombinant heparanase by MDA cells. The relevance of this finding to breast cancer progression is being investigated.

To further elucidate the significance of heparanase in breast cancer, we applied a ribozyme (RNA molecule with sequence-specific endonucleolytic activity) targeting approach to suppress heparanase expression in breast carcinoma cells (*task 3)*. A pronounced reduction in heparanase activity and basement membrane (Matrigel) invasion was observed in MDA-435 cells transfected with the appropriate ribozyme construct. Studies are underway to sustain this effect over time and analyze the effect *in vivo*. We are also trying to adopt the small interfering RNA (siRNAs) approach, using the recently described pSUPER vector for a persistent suppression of heparanase gene expression. This vector was kindly provided to us by Dr. R. Agami (Science, 296: 550-553, 2002).

In continuation of our effort to design heparanase-inhibiting species of oligosaccharides (i.e., heparin, laminaran sulfate) we established a collaborative research with Dr. Benito Casu (G. Ronzoni Research Institute, Milan, Italy) and have already identified lead inhibitory compounds (*task 3)*. Our goal is to determine the minimal length of oligosaccharide and level of sulfation required for efficient inhibition of heparanase activity, tumor angiogenesis and metastasis. We plan to further improve the molecular flexibility and biological interactions of heparin and laminaran sulfate, applying controlled glycol-splitting and sulfation/desulfation strategies. We also plan to modify selected heparanase-inhibiting oligosaccharides by mimicking the critical heparanase cleavable glycosidic C-O-C bond with resistant C-S-C or C-C bonds. The effect of these compounds will be studied *in vivo*, using the heparanase dependent system, described above, of breast carcinoma cells over-expressing secreted heparanase.

**"So what":** The results obtained thus far clearly support the originally proposed involvement of heparanase in breast carcinoma progression. A conclusive indication is the accelerated angiogenesis and growth of tumors produced by MCF-7 cells over-expressing the human heparanase cDNA and even more so the secreted form of the enzyme. Translocation of heparanase from the cytoplasm to the cell surface and its secretion appear to play an important role in its involvement in breast cancer progression. Of high significance is the potential regulatory effect of estrogen on heparanase promoter activity, cellular content and secretion. We have also demonstrated that estrogen promotes angiogenesis induced *in vivo* by MCF-7 cells embedded in Matrgel gel. A potent pro-angiogenic response was also observed in mammary glands of pregnant mice over-expressing the heparanase gene. Angiogenesis is being evaluated by non-invasive MRI analysis of vascular density, functionality and maturation. Progress was made in characterization of a proteolytic activity expressed by breast carcinoma cells and involved in processing and activation of latent heparanase. This protease is being purified and will then serve as a complementary target for identification and development of inhibitory molecules. Lead heparanase-inhibiting species of heparin and laminaran sulfate were prepared and characterized. Their efficacy in experimental models of breast carcinoma progression is being evaluated, using cells over-expressing the newly identified secreted form of heparanase. We are also applying ribozymes and siRNAs for a persistent suppression of heparanase gene expression both *in vitro* and *in vivo*.

**References**


1. Kennedy, A.R., and Wan, X.S. (2002). Effects of the Bowman-Birk inhibitor on growth, invasion, and clonogenic survival of human prostate epithelial cells and prostate cancer cells. Prostate, 50:125-133.

2. Zhang, M., Volpert, O., Shi, Y.H., and Bouck N. (2000). Maspin is an angiogenesis inhibitor. Nat. Med., 6, 196-199, 2000.

3. Shi, H.Y., Zhang, W., Liang, R., Abraham, S., Kittrell, F.S., Medina, D., and Zhang, M. (2001). Blocking tumor growth, invasion, and metastasis by maspin in a syngeneic breast cancer model. Cancer Res., 61, 6945-1651.

4. Goldshmidt, O., Zcharia, E., Aingorn, H., Guatta-Rangini, Z., Atzmon, R., Michal, I. Pecker, I., Mitrani, E., and Vlodavsky, I. (2001). Expression pattern and secretion of human and chicken heparanase are determined by their signal peptide sequence. J. Biol. Chem. 276: 29178-29187.

5. Abramovitch, R., Frenkiel, D., and Neeman, M. (1998). Analysis of subcutaneous angiogenesis by gradient echo magnetic resonance imaging. Magn Reson Med, 39: 813-824.

6. Goldshmidt, O., Zcharia, E., Abramovitch, R., Metzger, S., Guatta-Rangini, Z., Aingorn, H., Friedmann, Y., Mitrani, E., and Vlodavsky, I. (2002). Cell surface expression and secretion of heparanase markedly promote tumor angiogenesis and metastasis. PNAS. In press.

7. Elkin, M., Ilan, N., Ishai-Michaeli, R., Friedmann, Y., Papo, O., Pecker, I., and Vlodavsky, I. (2001). Heparanase as mediator of angiogenesis: mode of action. Faseb J, 15: 1661-1663.

8. Rochefort, H., Liaudet, E., and Garcia, M. (1996). Alterations and role of human cathepsin D in cancer metastasis. Enzyme Protein, 49: 106-116.

9. Mathieu, M., Vignon, F., Capony, F., and Rochefort, H. (1991). Estradiol down-regulates the mannose-6-phosphate/insulin-like growth factor-II receptor gene and induces cathepsin-D in breast cancer cells: a receptor saturation mechanism to increase the secretion of lysosomal proenzymes. Mol. Endocrinol., 5(6):815-822.

10. Laurent-Matha, V., Farnoud, M.R., Lucas, A., Rougeot, C., Garcia, M., and Rochefort, H. (1998). Endocytosis of pro-cathepsin D into breast cancer cells is mostly independent of mannose-6-phosphate receptors. J Cell Sci., 111:2539-2549.

11. Ward, T.H., Polishchuk, R.S., Caplan, S., Hirschberg, K., Lippincott-Schwartz, J. (2001). Maintenance of Golgi structure and function depends on the integrity of ER export. J. Cell Biol., 155, 557-570.

12. Zcharia, E., Metzger, S., Chajek-Shaul, T., Friedmann, Y., Pappo, O., Aviv, A., Elkin, M., Pecker, I., Peretz, T. & Vlodavsky, I. (2001). Molecular properties and involvement of heparanase in cancer progression and mammary gland morphogenesis. J. Mammary Gland Biol. Neoplasia, 6, 311-322.

**Appendix** (figures & figure legends)

**Figure legends**

**Figure 1.** Processing and activation of latent heparanase by MDA-435 cells. Recombinant latent 65 kDa heparanase (lane 1) was incubated (1 h, 37°C) with: **A.** a cytosol fraction of MDA-435 cells, and **B.** MDA-435 membrane fraction. Processing of the latent enzyme into the 50 kDa enzyme (arrow) and other proteolytic fragments is shown in lanes 2. Heparanase activity of the latent (□, 1 ) and processed (▲ , 2) enzymes was determined using either sulfate labeled ECM (**A**), or beads conjugated to labeled heparan sulfate (**B**).

**Figure 2.** Processing and activation of latent heparanase by MDA-435 cells. **A.** Recombinant latent 65 kDa heparanase (lane 1) was incubated (1 h, 37°C) with a cytosol fraction of MDA-435 cells in the absence (lane 2) and presence of PMSF (lane 3, compete inhibition of processing) or BBI (lane 4). BBI inhibits degradation of the enzyme by serine proteases, but not its conversion into the active 50 kDa heparanase. **B.** Left: a cytosol fraction of MDA-435 cells (lane 1) was first incubated with heparin-Sepharose beads. The beads were washed and incubated with recombinant latent 65 kDa heparanase in the absence (lane 2) or presence of BBI (lane 3). Heparanase activity in the respective systems [i.e., cytosol alone (1), latent enzyme processed in the absence (2) or presence (3) of BBI] was determined using beads conjugated to labeled heparan sulfate.

**Figure 3.** Processing and activation of latent heparanase is inhibited by maspin. Recombinant latent 65 kDa heparanase (lane 1) was incubated (1 h, 37°C) with a cytosol fraction of MDA-435 cells in the absence (lane 2) and presence (lane 3) of maspin. Conversion of the 65 kDa latent enzyme into a 50 kDa active heparanase is inhibited in the presence of maspin.

**Figure 4. Overexpression of secreted heparanase accelerates tumor growth and promotes tumor angiogenesis.** Female CD1 nude mice were inoculated (into the mammary gland) with *hpa*-transfected MCF7 breast carcinoma cells. **A. MRI analysis of vessel functionality and maturation.** Tumor bearing mice were imaged on day 30 after cell inoculation. Representative axial gradient echo images of MCF7 tumors produced by Chk-*hpa*- (top) and H-*hpa* (bottom) transfected cells are presented in the left panels. Increased tumor growth is demonstrated (the tumor is marked by a yellow circle). Functionality and maturation of the vasculature were derived from gradient echo images acquired during inhalation of air, air-$CO_2$ and carbogen. Color-coded VF and VD maps were derived and overlaid (VF>0.005; VD >0.005, see color scale) on the original coronal images. Note the increased vessel functionality (VF) and maturation (VD) in tumors produced by Chk-*hpa*- (top) vs. H-*hpa* (bottom) transfected MCF7 cells. **B. Vessel functionality (VF) and maturation (VD).** The mean ± SD values of VF and VD were calculated from the region of interest containing the whole tumor, applying 2 mice per group and 3 slices/mouse.

**Figure 5.** Tissue sections of primary tumors produced by Chimeric-*hpa*- vs. H-*hpa*- transfected MCF-7 cells expressing secreted vs. non-secreted forms of heparanase. Female athymic nude mice at 6-8 weeks of age were pre-implanted subcutaneously with 1.7 mg of 17 β-estradiol pellets (60-day release). Two groups of mice (6 mice each) were then injected into the mammary pads with $1x10^7$ MCF-7 cells (pooled population) stable transfected with either the H-*hpa* (non-secreted) (A), or chimeric-*hpa* (secreted) (B-D) cDNA. Intense neovascularization (high vascular density) is seen in the vicinity of tumors produced by MCF7 cells expressing the secreted enzyme vs. little angiogenesis of tumors produced by cells expressing the mostly intracellular human heparanase.

**Figure 6.** Effect of estrogen on heparanase mRNA expression. Estrogen depleted MCF-7 (A), or MDA-231 (B) cells were treated (24 h, 37°C) with estrogen ($1 \times 10^{-9}$M) in the absence and presence of the estrogen specific antagonist ICI128 ($1 \times 10^{-7}$M). The cells were then subjected to RNA extraction and quantitative RT-PCR, using heparanase and GAPDH specific primers.

**Figure 7. Effect of estrogen on cellular expression and secretion of heparanase by MCF-7 cells transfected with Chk-*hpa* or chimeric-*hpa* vs. mock transfected cells. A. Heparanase activity.** MCF-7 cells transfected with Chk-*hpa*, chimeric-*hpa*, or mock transfected were incubated for 2 h in serum free RPMI medium with (▲), or without (○) $10^{-8}$ M estrogen. The conditioned medium was then collected and incubated (24 h, pH 6.0, 37°C) with sulfate labeled ECM. Labeled degradation fragments released into the incubation medium were analyzed by gel filtration on sepharose 6B. **B. Immunostaining.** MCF-7 cells were seeded on glass coverslips in 4 well plates in RPMI medium without phenol red. Twenty four h later, estrogen ($10^{-8}$ M) was added for 2 hours to some of the wells (lower panels). Cells incubated in the absence of estrogen are presented in the upper panels. Plates were washed twice with PBS and fixed with 100% chilled methanol for 3 min. Cells were subjected to indirect immunofluorescence staining with monoclonal anti-heparanase antibodies (mAb-130) followed by C-3 conjugated gout anti mouse antibodies.

**Figure 8.** Effect of estrogen on breast carcinoma angiogenesis. Ovarectomized female CD1 nude mice were divided into two groups (n=5). The mice of one group (**b** & **d**; estrogen) were pre-implanted subcutaneously with 1.7 mg of 17 β-estradiol pellets (60-day release). Control mice (**a** & **c**, placebo) were not exposed to estrogen. Mice were then injected (s.c) with 0.4 ml cold Matrigel premixed with $5x10^6$ MCF-7 breast carcinoma cells. After 7 days, the mice were scarified, and the Matrigel plugs were removed and photographed (a & b). Sections were subjected to Mallory staining of blood vessels (c & d) and microscopic determination of vascular density (e).

**Figure 9**. Immunogold labeling of heparanase in human breast carcinoma cells. Cultured MCF-7 (A-C) and MDA-231 (B) cells were processed for transmission electron microscopy and heparanase was visualized using anti-human heparanase mAb 130 followed by anti-mouse IgG conjugated gold particles. Heparanase (arrows) is localized in lysosomes (A & B), the Golgi apparatus (C), and coated pits (D). Bar = 200 nm (A & D) and 100 nm (B & C).

**Figure 10.** Heparanase is localized in acidic vesicles. Localization of endogenous heparanase in MCF-7 **(A)** and MDA-231 **(B)** human breast carcinoma cells. Left: Cells stained with anti-heparanase antibodies (mAb 130) followed by Alexa-conjugated goat-anti-mouse antibody (green fluorescence). Middle: cells live-stained with LysoTracker, (red fluorescence). Right: Cells were labeled with LysoTracker followed by staining with anti-heparanase antibodies. Note the co-localization of heparanase and acidic vesicles (yellow fluorescence).

**Figure 11**. Heparanase activity depends on the integrity of the Golgi apparatus. **A**. Effect of pretreatment with Brefeldin A (BFA) on heparanase activity. Cultured MCF7 (left) and MDA-231 (right) cells were incubated (16 h, $37^0$C) in the absence (●), or presence of 0.1 (▲), 1 (□), or (△) 10 μg/ml Brefeldin A. The cells were dissociated with trypsin/EDTA, lysed by 3 cycles of freezing and thawing and incubated (24 h, pH 6.0, 2 x $10^6$ cells) with $^{35}$S-labeled ECM. Labeled degradation fragments released into the incubation medium were analyzed by gel filtration on Sepharose 6B.

**Figure 12.** Morphological appearance of mammary glands from control vs. *hpa*-transgenic pregnant mice. **A**. Whole mount of mammary glands derived from 14 days pregnant mice [left panels: over branching of ducts in the transgenic mice is marked by arrows, in comparison with mammary glands of control mice; Right panels: a high magnification of whole mounts derived from control (top) vs. *hpa*-transgenic (bottom) mice]; **B-D.** tissue sections of the same whole mount preparations derived from control (left) vs. *hpa*-transgenic (right) mice. **B.** Masson-trichrom staining. Basement membrane collagen stained blue with Masson-trichrome reagent ; **C.** Heparanase immunostaining. Sections stained with anti-heparanase antibodies (p9) cross-reacting with both the human and mouse enzymes; **D.** Sections stained with anti-smooth muscle cell (SMC) actin antibodies, staining mature blood vessels and myoepithelial cells.

**Figure 13.** Effect of ribozymes on heparanase RNA and activity. **A.** Short (~ 25 bp, top, left) and almost full-length (~1500 bp, bottom, left) heparanase RNA sequences were incubated (15 – 60 min) *in vitro* with different ribozymes and subjected to PAGE. Cleavage of the heparanase RNA is clearly seen upon incubation with ribozyme # 4, 6, 7 and 8. A marked suppression of heparanase activity was notes in MDA- 435 breast carcinoma cells stable transfected with ribozyme # 8 (top, middle). RT-PCR (top, right): MDA-435 cells, stable transfected with ribozyme #8 or mock transfected, were subjected to RT-PCR using H-*hpa* specific primers. Lane 1: human heparanase (H-*hpa*); Lane 2: GAPDH; Lane 3: - RT. **B.** Inhibition of cell invasion by *hpa*-ribozyme. A marked inhibition of Matrigel invasion was obtained in MDA-435 cells stable transfected with ribozyme # 8 (middle) vs. no inhibition in mock tranfected cells (left), or cells transfected with control inactive ribozyme (CRz; right).

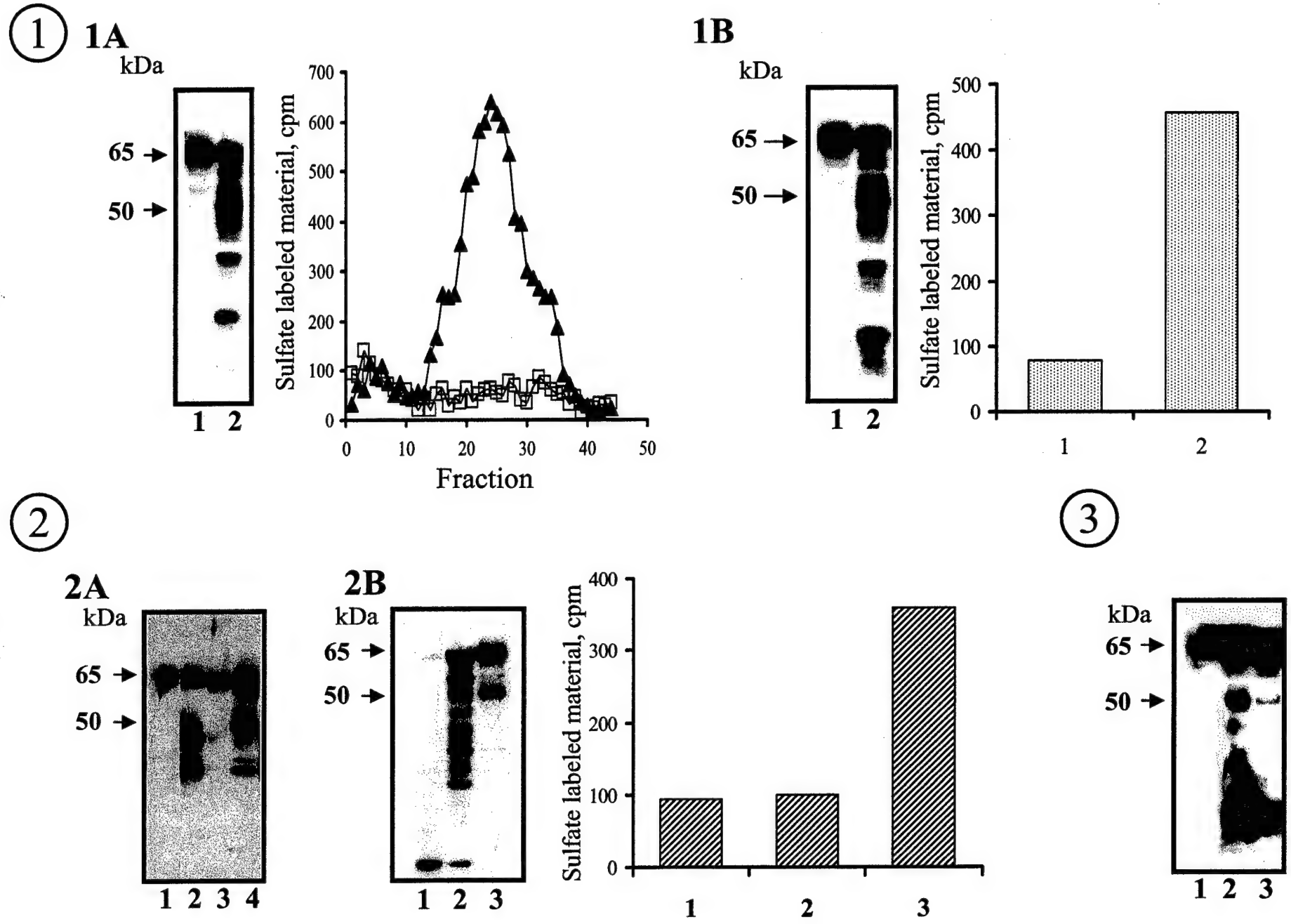
1
1A
kDa
65
50
1 2
Sulfate labeled material, cpm
700
600
500
400
300
200
100
0
0 10 20 30 40 50
Fraction
1B
kDa
65
50
1 2
Sulfate labeled material, cpm
500
400
300
200
100
0
1 2
2
2A
kDa
65
50
1 2 3 4
2B
kDa
65
50
1 2 3
Sulfate labeled material, cpm
400
300
200
100
0
1 2 3
3
kDa
65
50
1 2 3

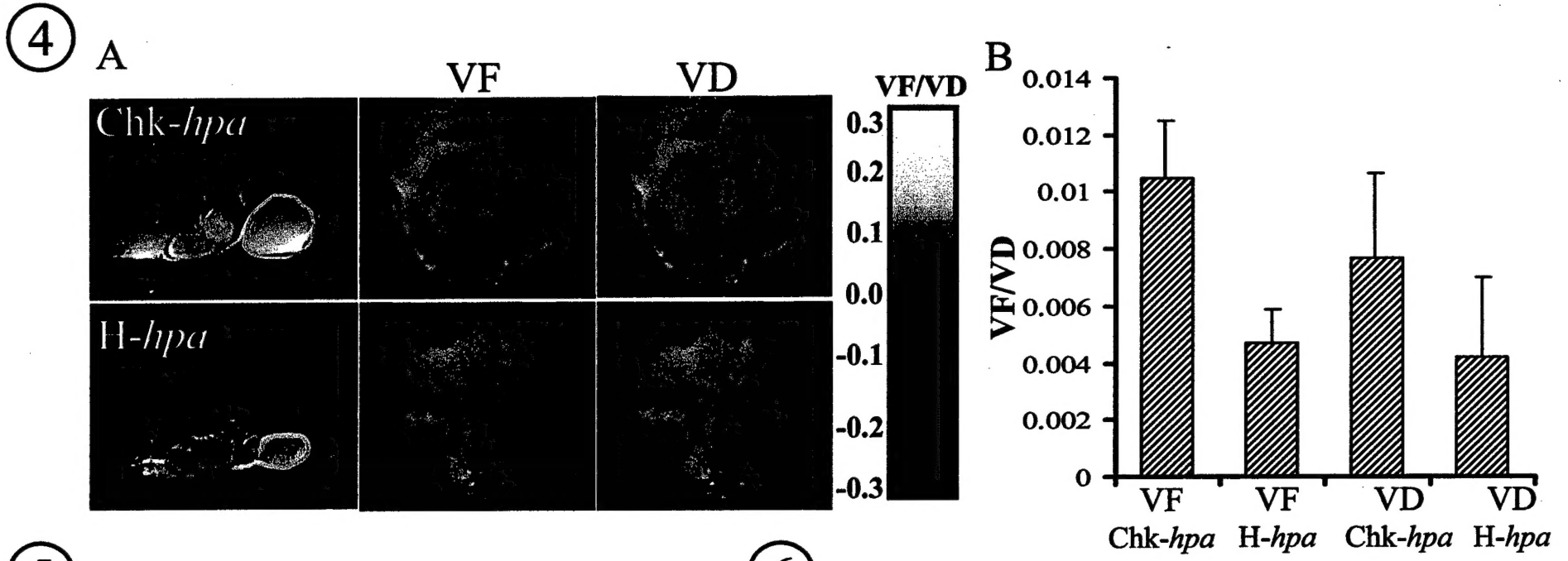
4
A
VF
VD
VF/VD
Chk-hpa
H-hpa
0.3
0.2
0.1
0.0
-0.1
-0.2
-0.3
B
0.014
0.012
0.01
0.008
0.006
0.004
0.002
0
VF/VD
VF
VF
VD
VD
Chk-hpa
H-hpa
Chk-hpa
H-hpa

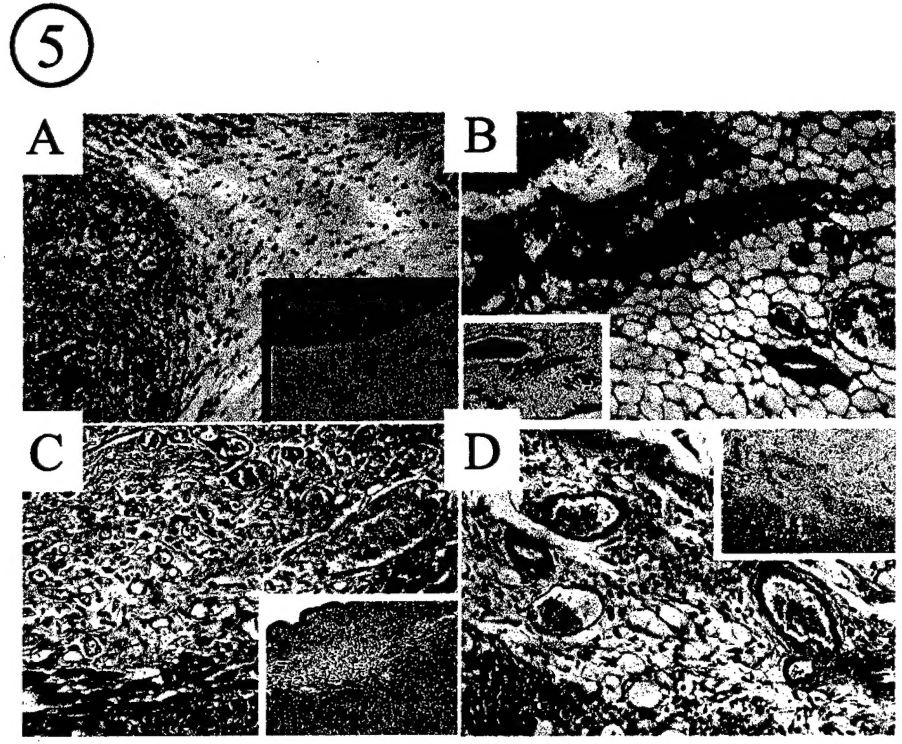
5
A
B
C
D

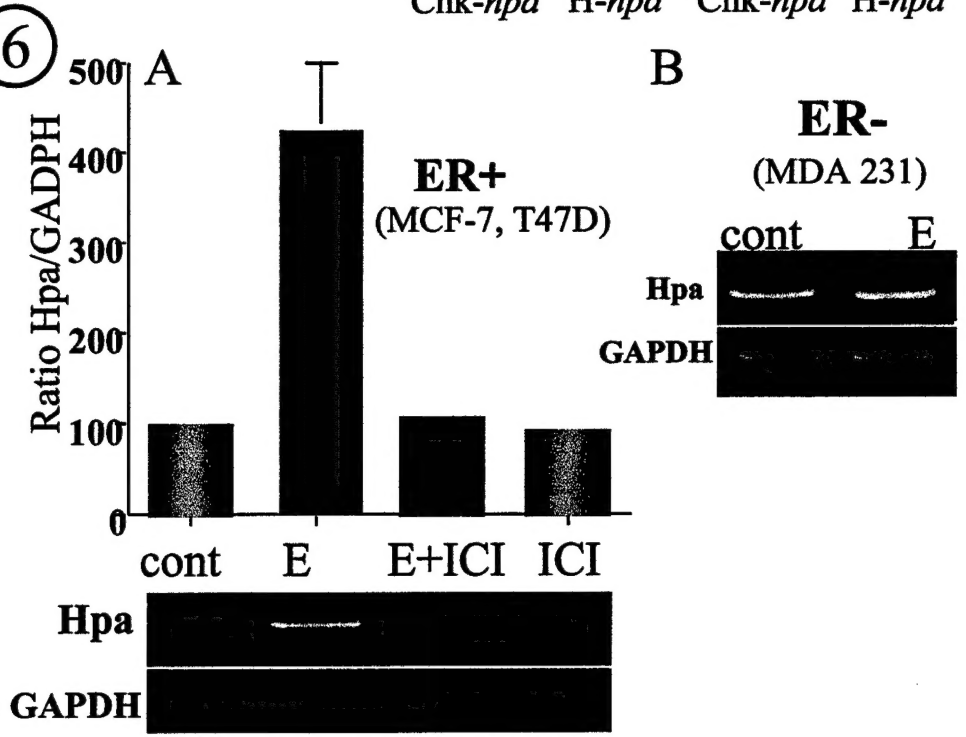
6
A
B
500
400
300
200
100
0
Ratio Hpa/GADPH
ER+
(MCF-7, T47D)
cont
E
E+ICI
ICI
Hpa
GAPDH
ER-
(MDA 231)
cont
E
Hpa
GAPDH

7

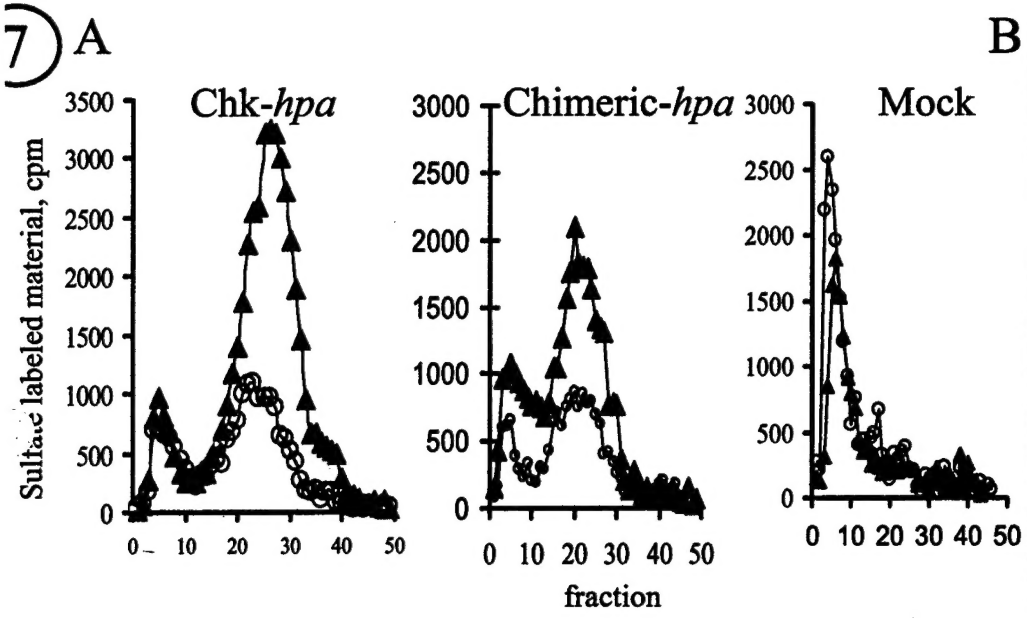
A
Chk-*hpa*
Chimeric-*hpa*
Mock
Sulfate labeled material, cpm
3500
3000
2500
2000
1500
1000
500
0
0 10 20 30 40 50
fraction

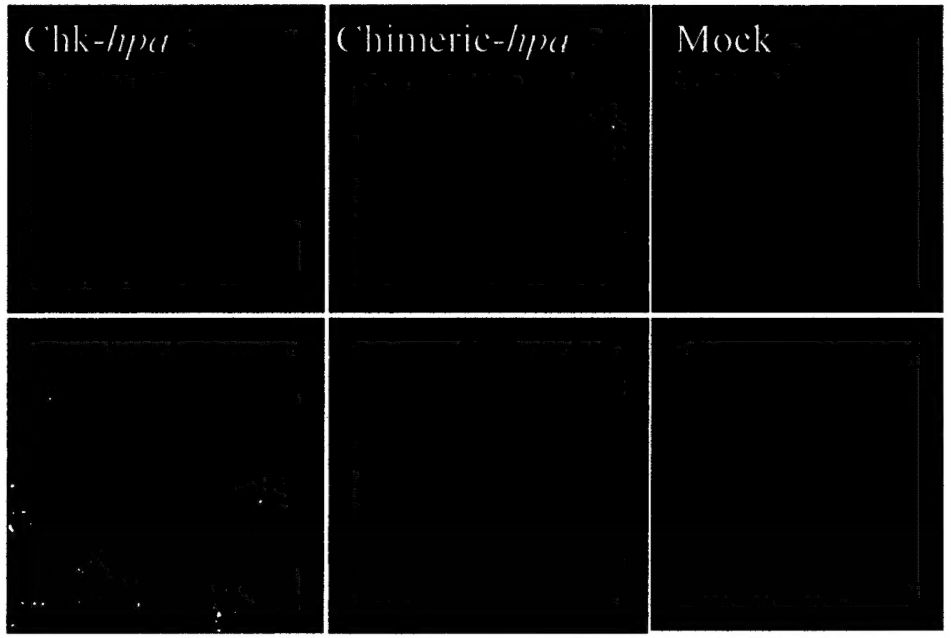
B
Chk-*hpa*
Chimeric-*hpa*
Mock

8

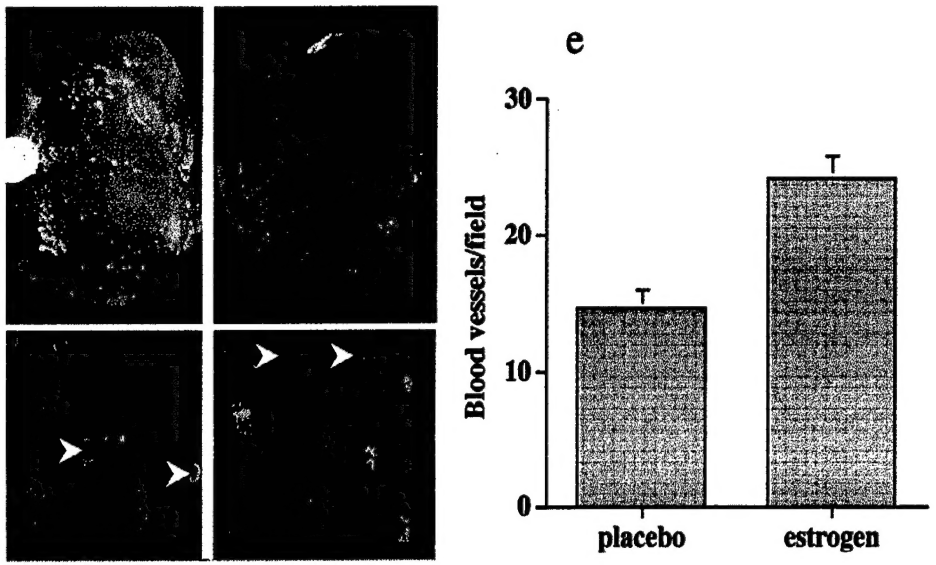
e
Blood vessels/field
30
20
10
0
placebo
estrogen

9

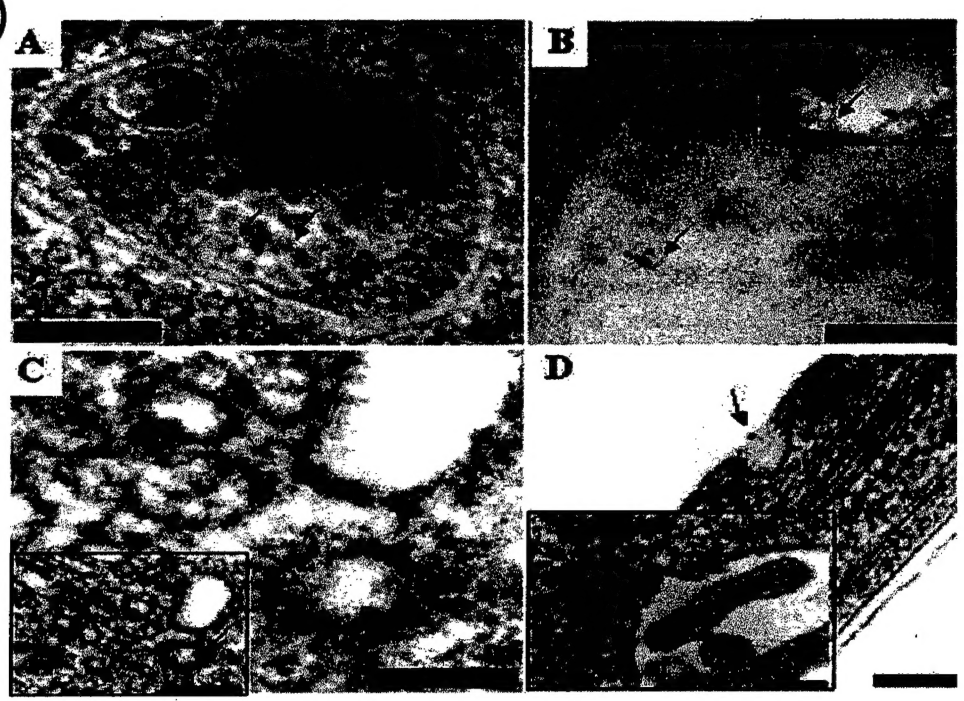
A
B
C
D

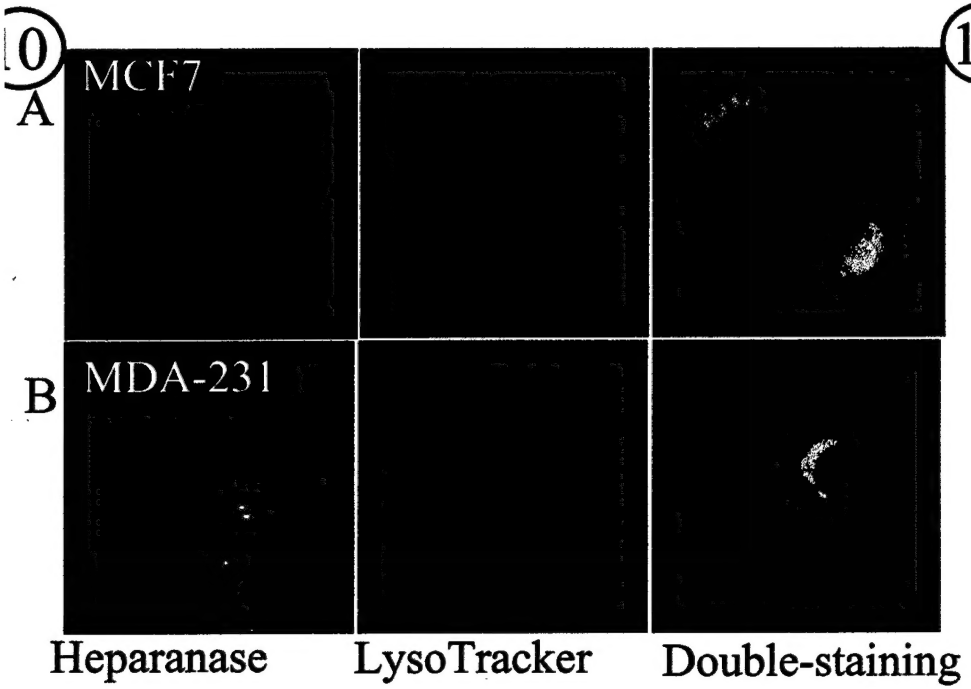
10
A
MCF7
B
MDA-231
Heparanase
LysoTracker
Double-staining

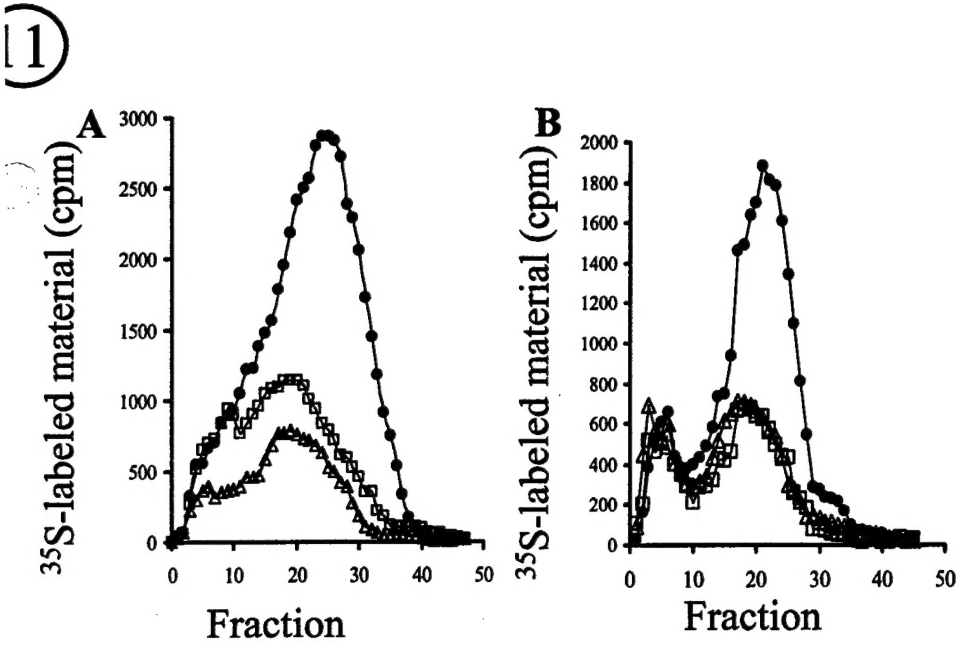
11
A
B
$^{35}$S-labeled material (cpm)
Fraction
0
500
1000
1500
2000
2500
3000
200
400
600
800
1200
1400
1600
1800
10
20
30
40
50

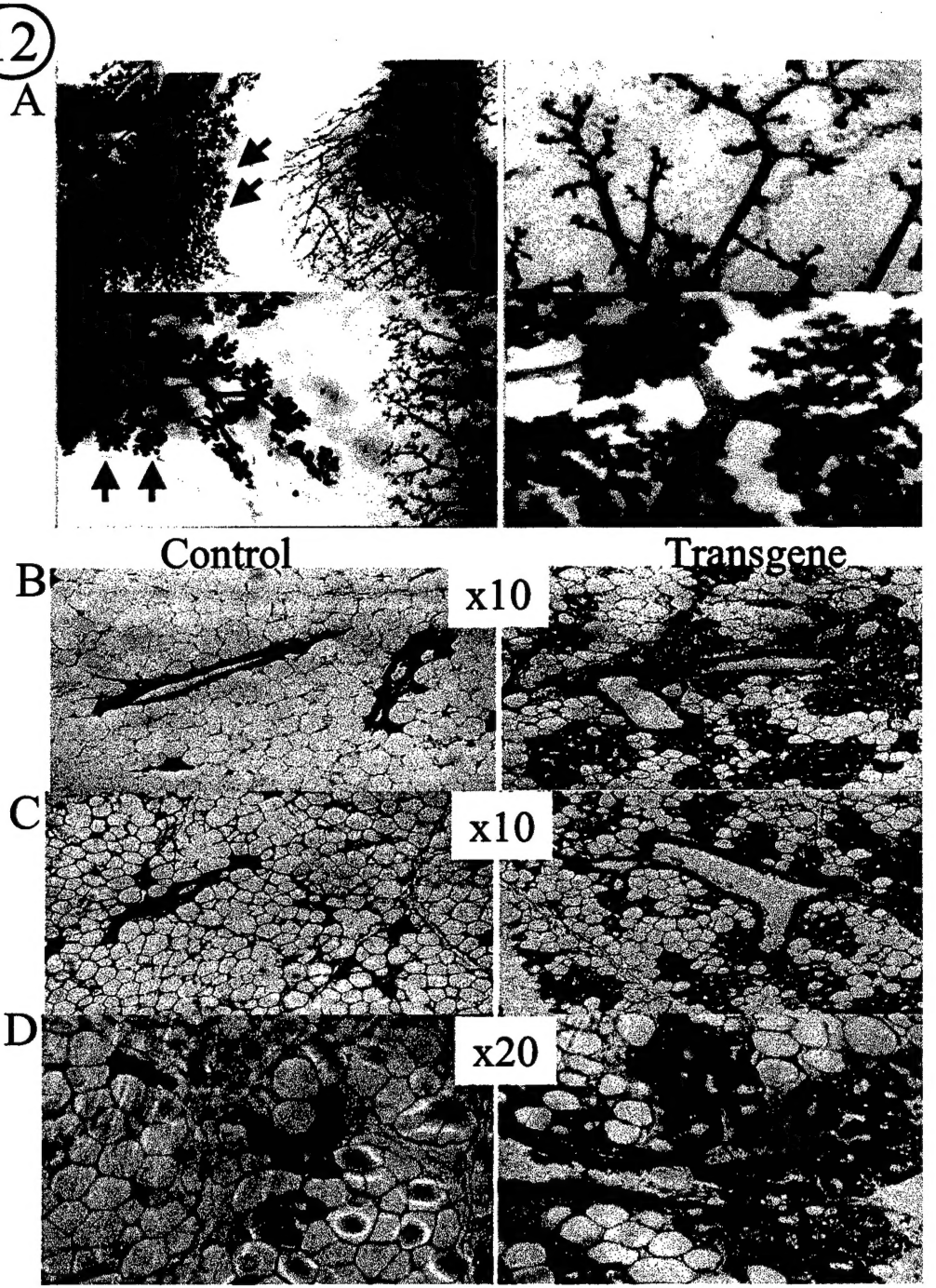
12
A
Control
Transgene
B
x10
C
x10
D
x20

13

# Effect of Ribozyme on heparanase RNA and activity

A

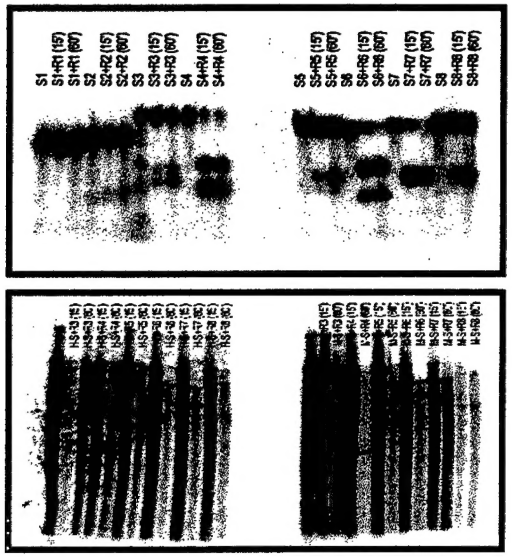

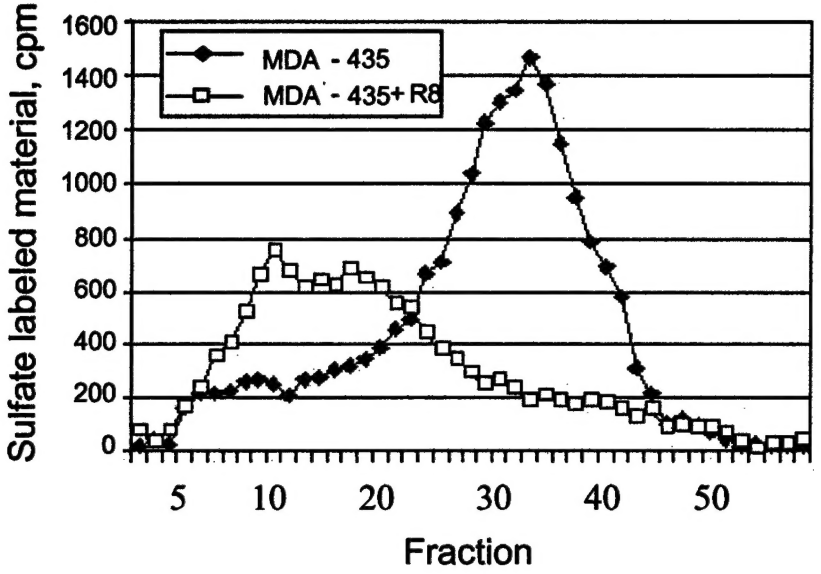


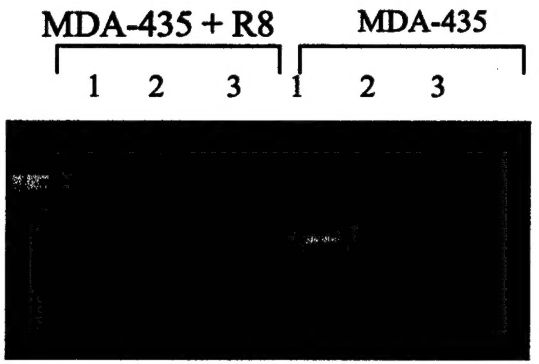


B

MDA-435 mock

MDA-435+Rz

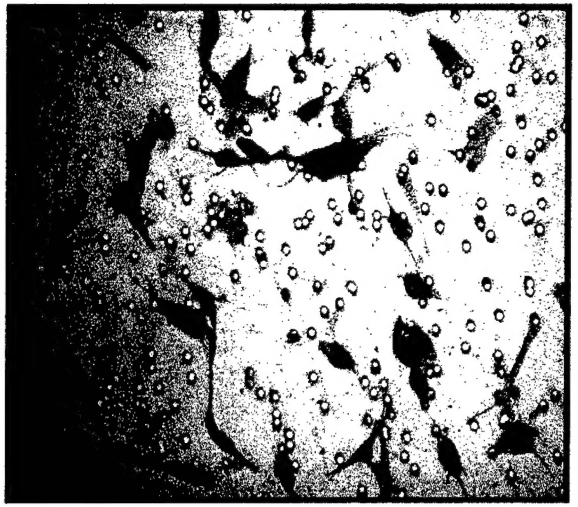

MDA-435+CRz